Latin American Journal of Energy Research - Lajer
periodicos.ufes.br/lajer

Latin American Journal of Energy Research – Lajer (2024) v. 11, n. 2, p. 161–175
https://doi.org/10.21712/lajer.2024.v11.n2.p161-175

Numerical modeling and experimental validation of a passive solar distillation of ethanol

Isadora Barbosa Silva[1], Érica Victor Faria[2], Nádia Guimarães Sousa[3], Kassia Graciele Santos[3,*]

[1] Engenheira Química, Universidade Federal do Triângulo Mineiro– UFTM, MG, Brasil
[2] Pesquisador, Universidade Federal do Espírito Santo – Ufes, campus São Mateus, ES, Brasil
[3] Professor do Curso de Engenharia Química, Universidade Federal do Triângulo Mineiro– UFTM, MG, Brasil
*Autor para correspondência, E-mail: kassia.santos@uftm.edu.br

Received: 12 September 2024 | Accepted: 18 December 2024 | Published online: 26 December 2024

Abstract: The increasing global demand for sustainable energy solutions highlights the potential of solar energy, a clean and abundant resource, for industrial processes such as distillation. This study investigates the passive solar distillation of ethanol mixed with a small fraction of oil, utilizing a phenomenological model validated against experimental data. Solar energy was employed to heat the mixture, capitalizing on its environmental benefits and cost-effectiveness, particularly in regions with high solar irradiation. Experiments were conducted with initial ethanol volumes of 500 mL, 750 mL, and 1000 mL, with temperature and distillate mass measured throughout the distillation process. The model accurately predicted the temperatures of the basin, ethanol, and glass cover, as well as the distillate mass, with prediction errors below 6%. Results indicate that solar radiation and wind speed significantly influence thermal efficiency, which ranged from 18.9% to 26%. It was achieved an average productivity of 4500 to 6500 mL/day·m² of distillate ethanol. The model's accurate predictions of distillate production demonstrate its potential as a valuable tool for optimizing passive solar distillation systems.
Keywords: numerical simulation; mass transfer; heat transfer, renewable energy, sustainable processes.

1 Introduction

Due to increasing global concerns over energy resources, various renewable energy generation methods have been explored to reduce costs, minimize environmental impact, and decrease the economic and energy dependency of non-fossil-fuel-producing countries. Despite its abundance and clean energy potential, solar energy remains underutilized. The solar energy received by the Earth annually is capable of meeting the world's energy demand thousands of times over (Villalva and Gazoli, 2012).

Brazil is almost entirely located in the intertropical region, thus receiving significant solar incidence throughout the year. The daily average irradiation over a year that occurs in any part of Brazilian territory ranges from 4.1 to 6.5 kWh/m². These values are higher than the irradiation received in countries that lead solar energy generation, such as Germany. Germany's sunniest region has a solar radiation index 40% lower than the index of Brazil's least sunny region (Cabral, 2013). According to the Ministry of Mines and Energy, in 2020, the installed capacity of photovoltaic solar energy in Brazil grew by 66%. However, given its potential, even though solar energy represents about 5% of the country's electricity matrix, there is a significant opportunity to exploit this resource further (GOV, 2021).

One practical application of solar energy is solar distillation. This process uses solar radiation to heat and change the phase of the more volatile liquid, enabling the separation of the mixture through evaporation, condensation, precipitation, and distillate capture. Solar distillation is being studied as an alternative to traditional distillation systems, particularly in regions with favorable technical conditions, such as air temperature, irradiation, relative humidity, and wind speed (Vasconcelos, 2015).

Solar distillation has been widely used for small-scale water purification, whether the water is saline or dirty, making it suitable for human and animal consumption. This method is not only effective but also employs clean energy, is accessible, economical, simple to maintain, and has no operating costs (Soares,

2004). Additionally, this method has been extensively studied and applied for the separation and purification of other liquids, such as solvents used in liquid-solid extraction.

There are several methods for oil extraction, including artisanal, mechanical, and solvent extraction. Silva et al (2019) conducted an experiment on coconut oil extraction using ethanol as a solvent, heated by solar energy. In their study, the extraction involved an organic solvent interacting with the plant matrix in a fixed bed, followed by oil and solvent separation through solidification and oil decantation after cooling. Subsequently, the ethanol containing oil residues was purified in a passive solar still to enhance the sustainability of the process.

A solar still is similar to a greenhouse and includes a container for the liquid, a transparent and inclined cover, and collection gutters. The container is painted black to promote greater absorption of solar energy and transfer it to the liquid. The cover is transparent and can be made of plastic or glass, with a preference for tempered or common glass, as water adheres better to it and does not fall back into the reservoir. This setup allows solar rays to enter, heating the solution until the more volatile liquid evaporates. The moist and hot vapor rises to the cover, which is at a lower temperature, and condenses. The inclination of the cover causes the condensed liquid to flow towards the gutters for collection (Bezerra, 2004; Maluf, 2005).

Scaling up this solar distillation process requires a thorough understanding of the heat and mass transfer phenomena within the still. Once a phenomenological model representing this operation is defined, it will be possible to propose new still geometries with higher productivity.

The literature includes some simplified models for passive solar distillation in equipment with various cover geometries. However, most applications focus on desalination or water purification. Therefore, validating the model for ethanol distillation is crucial, as well as determining the most suitable constitutive equations for heat transfer in this equipment geometry.

There are two types of solar distillation: passive and active. The direct system, also known as passive, is powered solely by solar radiation, whereas the indirect (active) system includes supplementary heat from another energy source. Despite offering lower yield, preference is given to the clean energy source, that is, passive solar distillation (Jorge, 2011).

Several factors influence the distillate rate, such as solar radiation, wind speed, ambient temperature, sky conditions (cloudiness), humidity, and design. The productivity of the still is directly linked to wind speed and the temperature in the tray (Gnanadason et al., 2011). For a 10°C increase in ambient temperature, from 23°C to 33°C, there is an 8.2% increase in still efficiency. If wind speed increases from 1 to 3 m/s, the still becomes 8% more efficient (Al-Hinai et al., 2002). However, not all solar energy incident on the still is used in the heat and mass transfer process. A significant portion is lost as some energy is dissipated, reflected, and absorbed by the glass cover, in addition to convection, radiation, and conduction processes (Freire de Sá, 2008).

According to Freire de Sá (2008), 39% of the incident solar radiation is dissipated by the glass, with 9% absorbed and 9% reflected. The liquid surface reflects 7%, the net radiation from the glass represents 5%, convection accounts for 6%, evaporation represents 19%, and losses through the still walls and thermal insulation amount to 13%, leaving only 32% as useful energy stored by the water.

Table 1 presents a comparison of the productivity of passive solar stills according to different authors. Moura (2019) examined various configurations of passive solar stills, considering factors such as location, solar radiation, cover thickness, tank lining or construction material, and the resulting distillate production. The study revealed that solar stills with cover thicknesses exceeding 4 mm yielded unsatisfactory results.

Vorayos et al. (2006) evaluated the performance and economic feasibility of continuous solar ethanol distillation systems using flat-plate and evacuated heat pipe solar collectors. Mathematical models for each system component were developed, and simulations showed good agreement with experimental data, within 14% accuracy. Starting with a 10% alcohol concentration, the simulation estimated a production yield of 12,500 liters per year of 80% alcohol.

Altarawneh et al. (2017) investigates the annual performance of single basin single slope, double slope, and pyramidal solar stills in Ma'an, Jordan, from January to December 2015. By testing various orientations and tilt angles (15°, 30°, and 45°) and developing mathematical models, it was found optimal tilt angles of 30.3° for single slope, 45° for double slope, and 65° for pyramidal stills. The single slope still showed a 28% productivity increase under optimal conditions. In summer, a south-oriented double slope still with a 35° tilt angle performed slightly better than other designs.

Mohsenzadeh et al. (2022) presented a transient model for a single slope single basin passive solar still, incorporating factors such as the evaporation chamber's aspect ratio, thermal inertia, and salinity levels. The model predicted a 5% higher performance compared to measurements. Findings included a 21% drop in glass transmissivity and greater water yield with a larger aspect ratio. They also reported the effects of

water depth and solar radiation on yield and emphasized the importance of thermal inertia for accurate predictions and optimization of passive solar stills.

Table 1. Comparison of passive solar still production (Moura, 2019).

Reference	Solar still specifications	Location	Solar Radiation (W/m²)	Production (Kg/dia.m²)
Tayeb (1992)	30 cm x 80 cm tank. Single slope glass cover.	Egypt	17000	0.313
Elkader (1998)	Single slope 35º glass roof, 3 mm thickness. 1 m² masonry tank.	Egypt	15700	5.6
Badran (2007)	Single slope 32º, 4 mm roof. 1 m² asphalt-lined tank	Jordan	1200	4.21
Tanaka (2009)	The roof was 5 mm thick glass (20º). 10º mirrored reflector. The basin (355 mm x 343 mm) had a wooden frame and was lined both with mirrored stainless steel sheets.	Japan	695	2.9
Panchal; Shah (2011)	Single slope 30º glass roof, 12mm thickness. 1 m² masonry tank	India	2700	0.58
	Single slope 30º glass roof, 12 mm thickness. 1 m² galvanized iron tank	India	2700	3.8
Luna (2016)	Double slope roof, 25º. Masonry and ferrocement tank, 1.20x2.30 m	Paraíba, Brazil	1827	3.28
Spirandeli et al. (2017)	Four-sided pyramidal roof, 19º. 1 m² aluminum tank	Uberaba, Brazil	3632	3.26
Raj; Manokar (2017)	Basin lined with an iron sheet at the bottom and a wooden frame, 0.5m x 1m. Single glass cover with a 10º inclination and 4 mm thickness.	Chennai, Índia	3264	3.43

Despite the significant advancements in solar distillation technology, there remains a notable gap in the development of comprehensive phenomenological models capable of accurately predicting the performance of solar stills under varying operational conditions. Most existing models primarily address water desalination, with limited focus on the distillation of other substances, such as ethanol contaminated with oil. Developing accurate predictive models not only advances scientific understanding but also supports practical applications by providing insights into system performance and enabling the design of more efficient and cost-effective solar distillation systems.

In this context, the main objective of this study was to validate a phenomenological model for the computational simulation of passive solar distillation of ethanol contaminated with a small fraction of oil. To achieve this, experimental data from three experiments conducted by Silva et al. (2019) were used. Constitutive equations were selected to represent heat exchanges. By knowing the equipment geometry and the meteorological and initial experimental conditions, the temperatures of the basin, liquid, and glass cover were calculated, as well as estimating the thermal efficiency of the still and the mass of distillate obtained during the experiments.

2 Methods

2.1 Passive solar distillation experimental unit

Figure 1 presents the experimental unit used by Silva et al. (2019), which features a glass distiller cover measuring 50x50x12 cm, with a double slope of 34°. It was equipped with eight aluminum channels inside the glass cover to facilitate the drainage of condensed liquid. The walls of aluminum base plate absorber, measuring 45x45x7 cm, were black painted to increase the solar absorptivity.

Insulation is provided by expanded polystyrene covered with matte black film. The distiller is supported by a wooden table. The temperature measurement was carried out using five thermocouples and one multimeter. Two ¼-inch diameter hoses, fixed with silicone adhesive at the ends of the distiller body, pass through holes made in both the aluminum basin and the table to collect the distillate in graduated glass containers.

Additional insulation was achieved by placing expanded polystyrene covered with matte black film between the table and the basin (in orange at Figure 1a). Silicone adhesive was also used along the edges of the glass cover to ensure proper sealing.

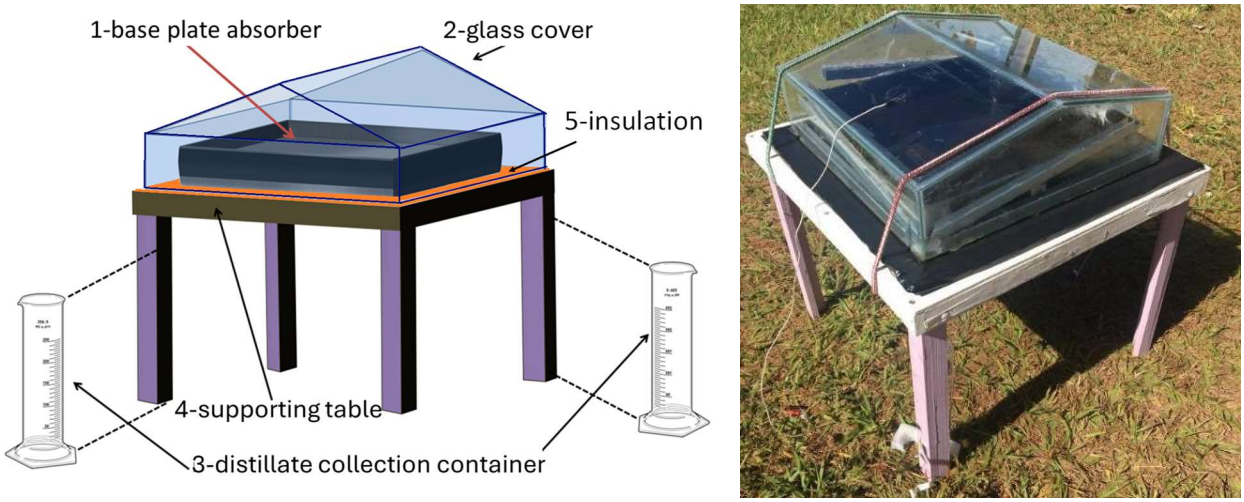

(a) (b)

Figure 1. Experimental unit of passive solar distillation.

2.2 Solar distillation experiments of Silva et al. (2019)

Silva et al. (2019) conducted batch mode experiments using three different initial volumes—500, 750, and 1000 mL. The distillation sample consists of a mixture of oil and alcohol at an oil concentration of 0.12%. So, for the simulations, this amount of oil was not considered.

The experiments were carried out on June 27, 28, and 30, 2017, under mild weather conditions with low cloud cover, all starting at 10:00 AM in Uberaba, MG, Brazil. Distillate volume and temperatures were measured every 30 minutes, including air temperature inside the distiller, temperatures on the inner and outer surfaces of the glass cover, the temperature of the inner basin wall, and the liquid within the basin. Meteorological factors, such as wind speed, solar radiation, and ambient temperature, were obtained hourly from the website of the National Institute of Meteorology (INMET) using data from the meteorological station located at the Univerdecidade Campus of UFTM – ICTE II, in Uberaba. Consequently, all experimental data were analyzed at 1-h intervals.

Thus, the relationship between incident solar radiation and heat transferred by evaporation-condensation determines the thermal efficiency of the distillation process (η). This can be calculated using Eq. (1) (Duffie and Beckman, 1991):

$$\eta = \frac{m_c L_w}{A_b \mathrm{I}} 100 = \frac{P_m L_w}{I} 100 \quad (1)$$

where m_c is the distillate production rate (kg.h^{-1}); L_w is the latent heat of vaporization of the liquid to be distilled (kJ.kg^{-1}); A_b is the effective area of the still basin (m²); I is the solar radiation received by the still during operation (kJ.m^{-2}.h^{-1}); and P_m is the mass productivity (kg. m^{-2}.h^{-1}). For the calculation of mass productivity, the density of ethanol was assumed to be 0.79 g·cm^{-3}.

2.3 Modelling and simulation

Figure 2 illustrates the thermal heat flows between the system components, while Figures 3 (a, b, and c) present the control volume schemes. These figures represent the energy balance used to derive the mathematical modeling equations for the distillation process (Mohsenzadeh et al., 2022).

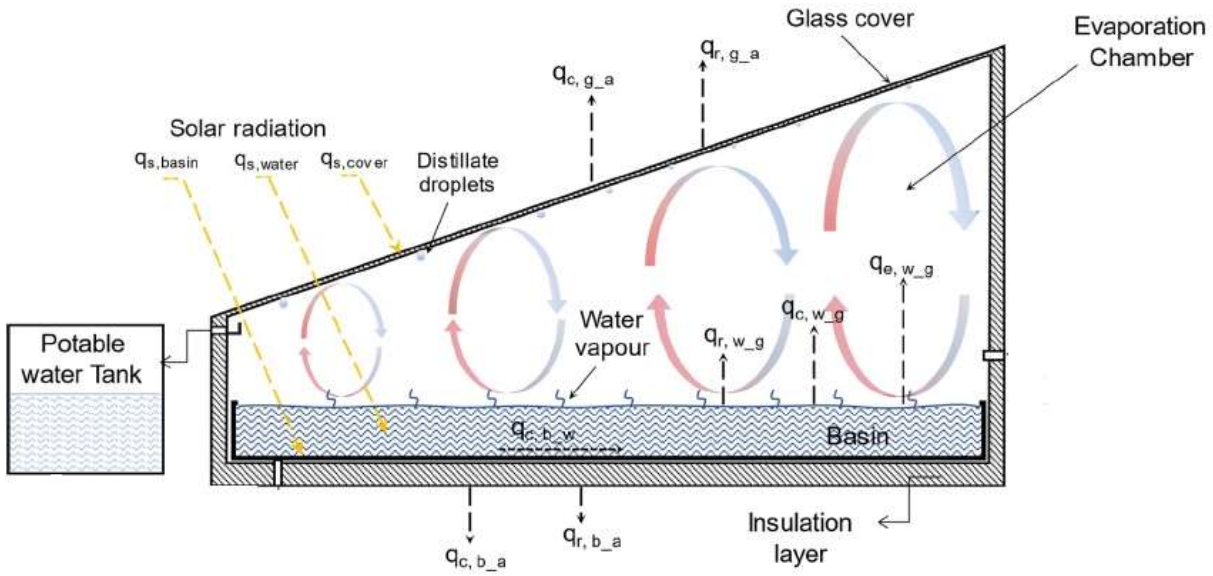

Figure 2. Thermal heat flows within the passive solar distiller. Source: Mohsenzadeh et al. (2022).

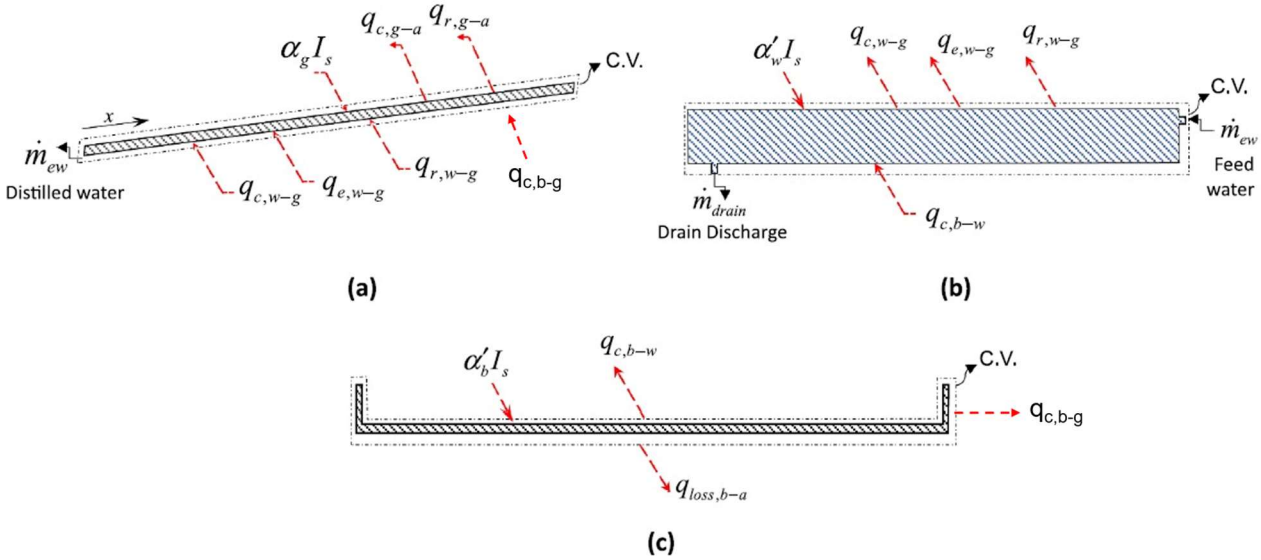

Figure 3. Control volume schemes indicating thermal heat flows: (a) glass cover, (b) ethanol volume, and (c) basin. Source Mohsenzadeh et al. (2022).

The following simplifying assumptions were adopted in the development of the model:

- The amount of oil in the mixture is negligible. Therefore, the physical and chemical properties of pure ethanol were used.
- The temperature gradient of the ethanol column within the basin was considered negligible, assuming a uniform temperature throughout the volume.
- No vapor leakage occurs from the solar distiller's evaporation chamber.
- The temperature is uniform across the glass cover.
- For heat exchange between the basin and the liquid, the properties of the liquid phase were applied.
- For heat exchange between the fluid and the glass, the properties of the vapor phase were used.
- The vapor phase temperature was calculated as the average between the liquid temperature in the basin and the glass temperature.

The studied distiller lacks thermal insulation between the basin and the distiller body, and thus, an energy transfer from the basin to the glass was included in the model.

Table 2 lists the constant parameter values and corresponding units used in the mathematical model simulation. Table 3 presents the ordinary differential equations (ODEs) for mass and energy balances in the basin, liquid film, and glass cover, while Table 4 shows the constitutive equations (Faria, 2015). Equations 2 to 5 represent the energy balances for each component of the distiller, as shown in Figure 3: the temperature of the basin or distiller base (Tb), the ethanol liquid film in the basin (Tw), the glass cover (Tg), and the mass of distillate (mc), respectively.

Table 2. Constant Parameters used in simulations.

Parameters	Value	Parameters	Value
Glass reflectivity, ρ_g	0.05	Thermal insulation thickness, x_{isol}	0.008 m
Glass absorptivity, α_g	0.09	Thermal conductivity of insulation, k_{isol}	0.01 W/mK
Ethanol absorptivity, αw	0.04	Volumetric thermal expansion coefficient, β	10.957 x10^{-4} 1/K
Distiller base absorptivity, α_b	0.984	Latent heat of vaporization, L_w	8.36 x105 J/Kg
Ethanol emissivity, ε_w	0.92	Average height of the distiller, L	0.145 m
Glass emissivity, ε_g	0.86	Distance between the basin side and the glass, l	0.01 m
Glass cover area, A_g	0.267 m^2	Stefan-Boltzmann constant, σ	5.67 x10-8 W/m^2K^4
Basin area, A_b	0.2025m^2	Acceleration due to gravity, g	9.81 m^2/s
Cover mass, M_g	3.34 Kg	Lateral area of the basin, AL_{bacia}	0.126 m^2
Base mass, M_b	0.652 Kg	Area of the base in contact with ethanol, A_s	0.2114 m^2
Specific heat of glass, Cp_g	1.8 J/KgK	Specific heat of base, Cp_b	0.473 J/KgK

Table 3. Mass and Energy Balance Equations in the Passive Solar still.

- Energy Balance in the Basin (Absorber Body)

$$m_b C_{pb}\frac{dT_b}{d_t} = Ia_b A_b - q_{c,b-w} - q_{c,b-g} - q_{loss} \quad (2)$$

- Energy Balance in the Ethanol Liquid Film in the Basin

$$m_{w_0} C_{pw}\frac{dT_w}{d_t} = Ia_w A_b + q_{c,b-w} - q_{r,w-g} - q_{c,w-g} - q_{qe,w-g} \quad (3)$$

- Energy Balance in the Glass Cover

$$m_g C_{pg}\frac{dT_g}{d_t} = Ia_g A_g + q_{r,w-g} + q_{c,w-g} + q_{c,b-g} + q_{e,w-g} - (q_{r,g-a} + q_{c,g-a}) \quad (4)$$

- Mass Balance of the Liquid in the Basin

$$\frac{dm_c}{d_t} = h_{evap}\frac{(T_w - T_g)}{L_{Tw}} \quad (5)$$

Table 4. Constitutive Equations Used in the Simulation of the Passive Solar still.

- Absorptances in the glass cover, liquid film, and basin, respectively

$$a_g = (1-\rho_g)\alpha_g \quad (6)$$

$$a_w = (1-\rho_g-\alpha_b)\alpha_w \quad (7)$$

$$a_b = (1-\rho_g-\alpha_b-\alpha_w)\alpha_b \quad (8)$$

- Heat transferred by convection from the basin to the ethanol

$$q_{c,b-w} = h_{c,b-w}(T_b - T_w)A_s \quad (9)$$

- Natural convection coefficient between the basin and the liquid (Incropera, 2008, eq. 9.30)

$$h_{c,b-w} = \frac{k_w}{L}0{,}54(Gr_b Pr)^{0{,}25} \quad (10)$$

- Heat transferred by convection from the basin to the side glass (Incropera, 2008, eq. 9.51)

$$q_{c,b-g} = \frac{k_{w_v}}{l}0{,}22\left(\frac{Gr_g {Pr_v}^2}{0{,}2+Pr_v}\right)^{0.28} * \left(\frac{0{,}45}{L}\right)^{-0{,}25} A_{lbacia}(T_b - T_g) \quad (11)$$

- Heat lost from the basin to the environment

$$q_{loss} = U_b A_b (T_b - T_a) \quad (12)$$

- Global heat transfer coefficient for losses from the basin to the environment

$$U_b = \left(\frac{x_{isol}}{k_{isol}} + \frac{1}{h_{c,b-a}}\right)^{-1} \quad (13)$$

- Heat transferred by radiation from ethanol to the glass

$$h_{c,b-a} = 5{,}7 + 3{,}8 * vento \quad (14)$$

- Heat transfer coefficient by radiation from ethanol to the glass (Faria, 2015)

$$q_{r,w-g} = h_{r,w-g}(T_w - T_g)A_g \quad (15)$$

- Coeficiente de transferência de calor por radiação do etanol para o vidro (Dunkle, 1961)

$$h_{r,w-g} = \varepsilon_{eff}\sigma({T_w}^2 + {T_g}^2)(T_w + T_g) \quad (16)$$

- Effective emissivity

$$\varepsilon_{eff} = \left(\frac{1}{\varepsilon_w} + \frac{1}{\varepsilon_g} - 1\right)^{-1} \quad (17)$$

- Heat transferred by convection from ethanol to the glass

$$q_{c,w-g} = h_{c,w-g}(T_w - T_g)A_g \quad (18)$$

- Convective heat transfer coefficient from ethanol to the glass

$$h_{c,w-g} = \frac{k_{w_v}}{L_c} 0{,}22 \left(\frac{Gr_g {Pr_v}^2}{0{,}2 + Pr_v}\right)^{0.28} * \left(\frac{0{,}45}{L}\right)^{-0{,}25} \quad (19)$$

- Evaporation heat

$$q_{e,w-g} = h_{evap}(T_w - T_g)A_g \quad (20)$$

- Heat transfer coefficient to the glass by evaporation (Faria, 2015)

$$h_{evap} = 16{,}273.10^{-3} h_{c,w-g} \left(\frac{P_w - P_g}{T_w - T_g}\right) \quad (21)$$

- Partial vapor pressures of ethanol between the liquid and cover glass

$$P_i = \left(10^{\left(5{,}24677 - \frac{1.598{,}673}{T_i - 46{,}424}\right)}\right) * 10^5 \quad (22)$$

- Heat transferred by radiation from the glass

$$q_{r,g-a} = h_{r,g-a}(T_g - T_{sky})A_g \quad (23)$$

- Atmospheric temperature

$$T_{sky} = 0{,}00552 {T_a}^{1{,}5} \quad (24)$$

- Radiative heat transfer coefficient of the glass

$$h_{r,g-a} = \varepsilon_{eff}\sigma({T_g}^2 + {T_{sky}}^2)(T_g + T_{sky}) \quad (25)$$

- Heat transferred by radiation from the glass to the environment

$$q_{r,g-a} = h_{c,g-a}(T_g - T_a)A_g \quad (26)$$

- Convective coefficient of the glass to the environment

$$h_{c,g-a} = 2{,}8 + 3 * vento \quad (27)$$

Table 5 outlines the initial conditions for volume (V_0), mass (M_0), and thickness (e_0) of the liquid layer in the experiments conducted by Silva et al. (2019). In this study, the liquid thickness was assumed constant throughout the experiment.

Table 5. Initial experimental conditions by Silva et al. (2019).

	Test 1	Test 2	Test 3
V_0 (mL)	1000	750	500
M_0 (kg)	0.798	0.59175	0.395
e_0 (cm)	0.494	0.370	0.247

For each simulation in the conditions of Table 4, the system of equations (consisting of ODEs and constitutive equations) was solved using the *Scilab* software with the *ODE function* from the ODEPACK package. To assess the model's fit to the experimental data, three statistical parameters were employed: R^2 (coefficient of determination), RMSE (root mean square error), and MAPE (mean absolute percentage error).

3 Results and discussion

Figures 5 through 7 present a comparison between experimental and simulated data for Tests 1 to 3, showing the data of temperatures, distillate mass, thermal efficiency and meteorological data.

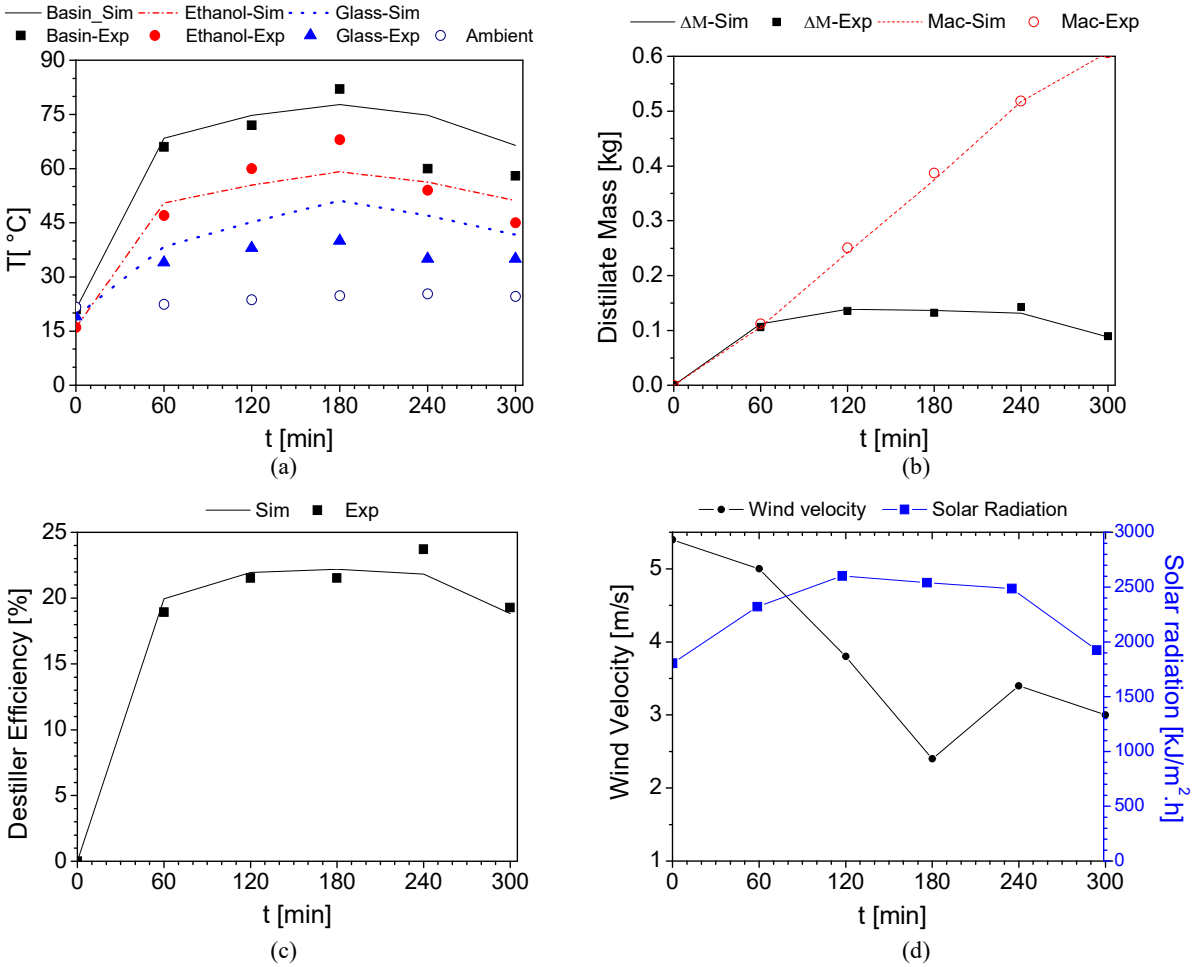

Figure 5. Comparison between experimental and simulated data for Test 1 (V0=1000 mL): (a) temperatures of the basin, ethanol, and glass cover; (b) mass collected at time intervals (ΔM), accumulated mass (Mac); (c) thermal efficiency; (d) wind speed and solar radiation.

During solar distillation, the black-painted basin acts as a solar radiation absorber, resulting in the highest temperature within the distiller (Figure 5a). As solar radiation increases, the heat absorbed by the basin also rises. The basin heats the fluid, promoting its evaporation and exhibiting the second highest temperature in the system (Figure 5b). Consequently, the partial pressure of ethanol within the distiller increases, as does the concentration of ethanol in the vapor phase. When ethanol vapor contacts the glass surface, it condenses, releasing heat and slightly warming the glass. The glass loses heat to the environment due to temperature differences and wind velocity, which increases the convective coefficient.

In Test 1 (V0 = 1000 mL), the final mass of distillate was 607.5 g over 5 h of distillation, while the model predicted 606.5 g, resulting in a prediction error of 0.33%, indicating high accuracy of the model in forecasting distillate production. Figure 5a compares experimental temperatures with those simulated in Test 1. The model captured the parabolic trend of temperature increases, although the last two points exhibited larger deviations, with temperature overestimations at the end of the experiment. Silva et al. (2019) reported significant cloud cover during the experiments, which impacted temperatures and explains the decrease in experimental basin temperature. The model does not account for cloud cover, resulting in similar behavior in Tests 2 and 3.

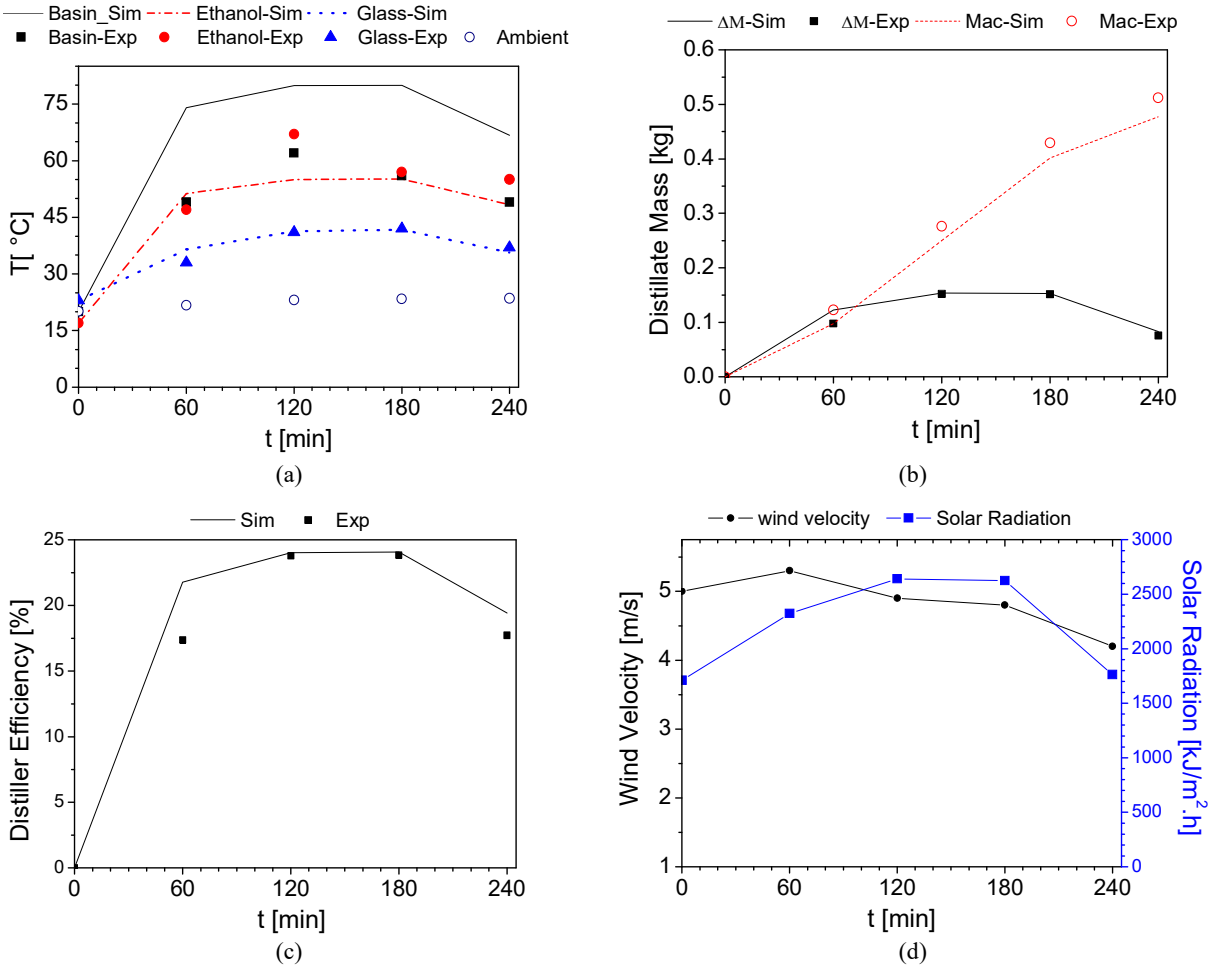

Figure 6. Comparison between experimental and simulated data for Test 2 (V0=750 mL): (a) temperatures of the basin, ethanol, and glass cover; (b) mass collected at time intervals (ΔM), accumulated mass (Mac); (c) thermal efficiency; (d) wind speed and solar radiation.

Figures 5d, 6d, and 7d highlight variations in meteorological data, estimated at 1-h intervals and collected approximately 1 km from the experiment site. Consequently, solar radiation and wind speed measurements may not precisely reflect experimental conditions due to the impact of clouds on these parameters. Another issue lies in the simplifying assumptions, as other energy losses from the system, such as those from the sealing rubber, were not considered. Additionally, the absorbance value for ethanol was not found and was thus assumed to be equal to that of water. These discrepancies directly affected the difference between experimental and simulated data, as shown in Figures 5b, 6b, and 7b, which depict the distillate mass collected each hour for each test.

Figures 5c, 6c, and 7c show the thermal efficiencies obtained during distillations, ranging from 18.9% to 26%. A parabolic pattern like the hourly collected distillate mass was observed. Mohsenzadeh et al. (2022) reported a thermal efficiency of 19.2% for a conventional single-slope still, similar to Alswat (2022), who achieved 25.31% in saline water distillation tests.

At several points, the simulated efficiency was overestimated, likely due to the high temperatures achieved in the simulations. Both simulated and experimental efficiencies are relatively low. According to Maluf (2005) this occurred possibly due to the reflection of incident radiation on the glass (10%), convection from the glass to the environment (12.2%), absorption in the glass (10%), radiation from the glass cover to the environment (3.7%), conduction from the container base (16%), and other heat losses (9.7%). So, only approximately 30% of the energy is effectively used as heat source for the phase change of the substance.

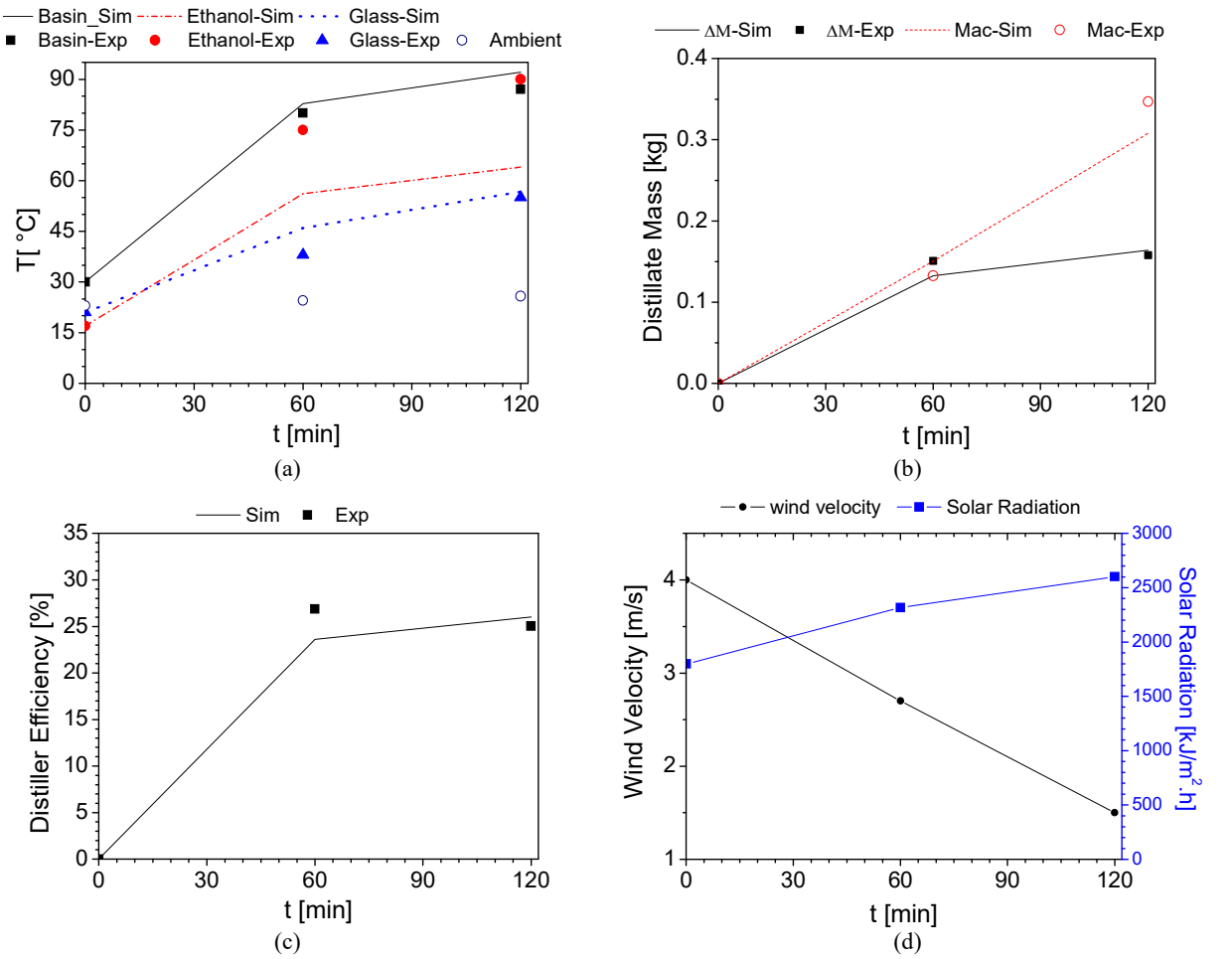

Figure 7. Comparison between experimental and simulated data for Test 3 (V0=500 mL): (a) temperatures of the basin, ethanol, and glass cover; (b) mass collected at time intervals (ΔM), accumulated mass (Mac); (c) thermal efficiency; (d) wind speed and solar radiation.

Figure 8 illustrates the effect of ethanol feed on the tray on the thermal efficiency (a) and the average distillate rate (a), for both experimental and simulated data. It can be observed that increasing the volume of ethanol on the tray leads to a reduction in the thermal efficiency of the distiller, which, in turn, impacts the reduction in the distillate rate. This can be explained due to enhanced sensible heat storage at increased ethanol mass within the solar still, as reported by Singh et al. (2024).

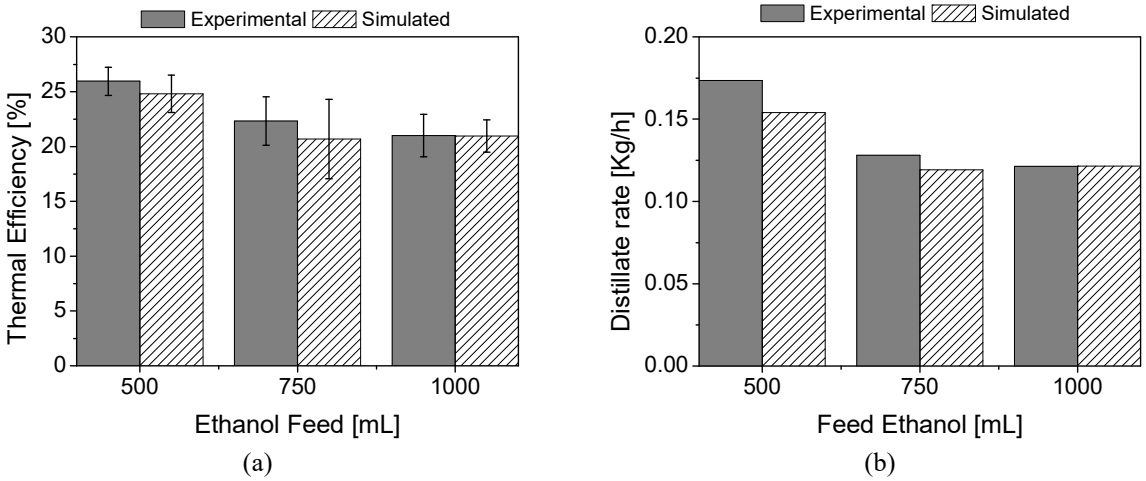

Figure 8. Effect of ethanol feed over the Thermal Efficiency (a) and mean Distillate rate (b).

Thus, it is expected that there may be an optimal amount of ethanol on the tray to maximize the distillate rate. Analyzing the data from Figure 9, we can observe the distillate volumetric productivity and

the residual liquid thickness in the basin as a function of solar radiation exposure time, for the experiments with ethanol feed of 500 mL (a), 750 mL (b) and 1000 mL (c). Comparing the current results with those reported in the literature, it is evident that the performance efficiency observed in this study is comparable. The thermal efficiency achieved in this work ranged from 21% to 26%, with an average productivity of 4500 to 6500 mL/day·m² of distillate ethanol. Maddah (2019) reported efficiencies ranging from 6% to 20.54% and a lower freshwater production rate of up to 446 mL/day·m², which is less than the rates reported in other studies, which achieved 4300 mL/day·m² (Al-Harahsheh et al., 2018), 3911 mL/day·m² (Singh et al., 2011) and 2595 mL/day·m² (Trieb, 2007) of water.

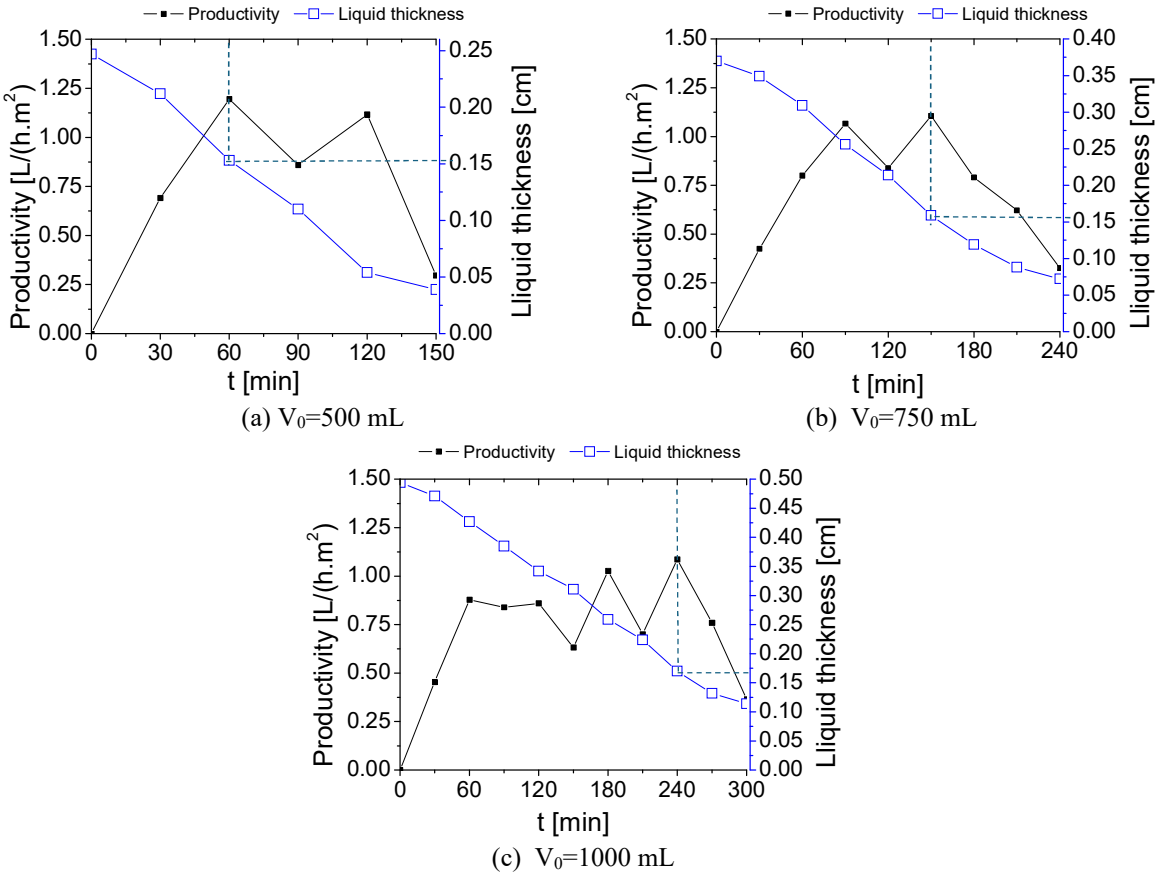

Figure 9. Effect of time of solar radiation exposure over the distillate productivity and the residual liquid thickness on the basin.

A linear reduction in the liquid thickness within the tank can be observed. However, it can also be noted that the liquid thickness on the tray at the point of maximum distillate productivity remains nearly constant, at approximately 0.16 cm. Therefore, one possible way to optimize the distillation process would be to maintain this thickness, which corresponds to 325 ml of liquid in the basin, through continuous feeding of the distiller, as demonstrated by Silva et al. (2019).

Table 6 presents the statistical values for comparison between experimental and simulated data of temperatures, the collected distillate mass, and the thermal efficiency of the solar still. The highest RMSE and MAPE values and the lowest R^2 values were found for temperatures due to unaccounted heat losses in the model and radiation and wind speed measurements that did not accurately represent the experimental conditions. The R^2 for the basin temperature (Tb) for 1000 mL was 99.6%, but the RMSE indicated an average error of 13.34% and the MAPE a mean difference of 15.24%.

Predictions for the collected distillate mass and the distiller efficiency were accurate, with determination coefficients (R^2) exceeding 97% for all volumes. The least satisfactory scenario was for 750 mL, with a MAPE of 6.116% and an RMSE of 2.669%. The distillate mass depends on the evaporation heat, which in turn depends on temperature variation, and the distiller efficiency depends on the distillate mass.

Table 6. Statistical evaluation of model fit quality for the responses: basin temperature (Tb), ethanol temperature (Tw), and glass temperature (Tg); distilled mass collected per hour (mc) and distillation thermal efficiency (η).

		Simulated variables				
Test	Parameters	T_b	T_w	T_g	m_c	η
1	RMSE	13.340	10.349	16.825	0.011	1.812
	R^2	0.996	0.973	0.857	0.998	0.997
	MAPE	15.240	7.655	18.757	3.446	3.446
2	RMSE	34.513	10.118	2.218	0.014	2.669
	R^2	0.805	0.955	0.997	0.999	0.992
	MAPE	37.380	7.063	2.611	6.114	6.116
3	RMSE	3.243	18.314	3.958	0.010	1.722
	R^2	0.993	0.852	0.995	0.993	0.991
	MAPE	2.789	9.007	4.018	2.665	2.661

4 Conclusion

The passive solar distillation of ethanol, as demonstrated in this study, provides a sustainable method for separating volatile mixtures using solar energy.

The phenomenological model developed was validated against experimental data, showing high accuracy in predicting temperature and distillate mass, with errors of less than 6%.

The thermal efficiency of the system was found to range between 18.9% and 26%, influenced by factors such as solar radiation and wind speed.

It was achieved an average productivity of 4500 to 6500 mL/day·m² of distillate ethanol.

Despite minor discrepancies in temperature predictions, the model offers significant potential for optimizing solar distillation systems.

Future research should focus on improving energy efficiency by reducing heat losses through better system insulation and material selection.

Nomenclature

A_b	Base area of the distiller	[m²]
A_{bacia}	Side area of the basin	[m²]
A_g	Glass cover area	[m²]
A_s	Base area in contact with ethanol	[m²]
Cp_b	Specific heat of the base	[J/kg·K]
Cp_g	Specific heat of the glass	[J/kg·K]
C_{pw}	Specific heat of ethanol	[J/kg·K]
$h_{c,b-g}$	Convective heat transfer coefficient between the basin and the glass	[W/m²·K]
$h_{c,b-w}$	Convective heat transfer coefficient between the basin and the ethanol	[W/m²·K]
$h_{c,g-a}$	Convective heat transfer coefficient from the glass to the environment	[W/m²·K]
$hc_{,w-}$	Convective heat transfer coefficient between the ethanol and the glass	[W/m²·K]
h_{evap}	Heat transfer coefficient to the glass by evaporation	[W/m²·K]
$h_{r,g-a}$	Heat transfer coefficient by radiation from the glass to the environment	[W/m²·K]
$h_{r,w-g}$	Heat transfer coefficient by radiation from ethanol to the glass	[W/m²·K]
I_{ab}	Solar irradiation on the base	[W/m²]
I_{ag}	Solar irradiation on the glass	[W/m²]
I_{aw}	Solar irradiation on the ethanol	[W/m²]
k_{isol}	Thermal conductivity of the insulation	[W/m·K]
k_w	Thermal conductivity of liquid ethanol	[W/m·K]
k_{wv}	Thermal conductivity of ethanol vapor	[W/m·K]
L	Average height of the distiller	[m]
L_{Tw}	Latent heat of vaporization of ethanol	[J/kg]
m_b	Mass of the basin	[kg]
m_c	Mass of the distillate	[kg]

m_g	Mass of the glass cover	[kg]
M_0	Initial mass of ethanol in the basin	[kg]
α_b	Absorptivity of the distiller base	[–]
α_g	Absorptivity of the glass	[–]
α_w	Absorptivity of ethanol	[–]
β	Volumetric thermal expansion coefficient	[1/K]
ϵ_{eff}	Effective emissivity	[–]
ϵ_g	Emissivity of the glass	[–]
ϵ_w	Emissivity of ethanol	[–]
ρ_g	Reflectivity of the glass	[–]
σ	Stefan-Boltzmann constant	[W/m²·K⁴]
t	Time	[s]
T_a	Ambient temperature	[°C]
T_b	Temperature of the basin or distiller base	[°C]
T_g	Temperature of the glass cover	[°C]
T_w	Temperature of the liquid ethanol film in the basin	[°C]
T_{sky}	Atmospheric temperature	[°C]
U_b	Overall heat transfer coefficient from the basin to the environment	[W/m²·K]
v	Wind speed	[m/s]
V_0	Initial volume of ethanol in the basin	[m^3]
$q_{c,b-g}$	Heat transferred by convection from the basin to the glass	[W]
$q_{c,b-w}$	Heat transferred by convection from the basin to the ethanol	[W]
$q_{c,g-a}$	Heat transferred by convection from the glass to the environment	[W]
$q_{c,w-g}$	Heat transferred by convection from the ethanol to the glass	[W]
q_{loss}	Heat lost from the basin to the environment	[W]
$q_{e,w-g}$	Heat of evaporation	[W]
$q_{r,g-a}$	Heat transferred by radiation from the glass to the environment	[W]
$q_{r,w-g}$	Heat transferred by radiation from ethanol to the glass	[W]
P_i	Partial vapor pressure	[Pa]
l	Distance between the side of the basin and the glass	[m]
x_{isol}	Thickness of the thermal insulation	[m]

References

Al-Harahsheh, M., Abu-Arabi, M., Mousa, H. and Alzghoul, Z. (2018). Solar Desalination Using Solar Still Enhanced by External Solar Collector and PCM. *Applied Thermal Engineering, 128*, 1030–1040. https://doi.org/10.1016/j.applthermaleng.2017.09.073.

Al-Hinai, H., Al-Nassri, M.S. and Jubran, B.A. (2002). Effect of climatic, design and operational parameters on the yield of a simple solar still. *Energy Conversion and Management, 43*, 1639–1650. https://doi.org/10.1016/S0196-8904(01)00120-0.

Alswat, M. (2022). Mathematical Modelling and Experimental Study of an Enhanced Double-Slope Glass Solar Still. *European Journal of Engineering and Technology Research, 7*(6). http://dx.doi.org/10.24018/ejeng.2022.7.6.2909.

Altarawneh, I., Rawadieh, S., Batiha, M., Al-Makhadmeh, L., Alrowwad, S. and Tarawneh, M. (2017). Experimental and numerical performance analysis and optimization of single slope, double slope and pyramidal shaped solar stills. *Desalination, 423*, 124–134. https://doi.org/10.1016/j.desal.2017.09.023.

Badran, O.O. (2007). Experimental study of the enhancement parameters on a single slope solar still productivity. *Desalination, 209*(1-3), 136-143. https://doi.org/10.1016/j.desal.2007.04.022.

Bezerra, M.A.S. (2004). Desenvolvimento de Um Destilador Solar Para Tratamento de Águas de Produção de Petróleo Com Vistas a Sua Utilização Na Agricultura e Geração de Vapor (in Portuguese). Mestrado em Engenharia Química, Universidade Federal do Rio Grande do Norte, Natal, RN.

Cabral, I.S. (2013). Energia solar – análise comparativa entre Brasil e Alemanha (in Portuguese). IV Congresso Brasileiro de Gestão Ambiental. Salvador, BA: Instituto Brasileiro de Ensino e Aperfeiçoamento em Saúde (IBEAS).

Duffie, J.A. and Beckman, W.A. (1991). *Solar Engineering of Thermal Process* (2nd ed.). New York: John Wiley & Sons.

Dunkle, R.V. (1961). Solar Water Distillation, the Roof Type Solar Still and Multiple Effect Diffusion Still. Developments in Heat Transfer, ASME, Proceedings of the International Heat Transfer, Part V, University of Colorado, Vol. 895.

Elkader, M.A. (1998). An Investigation of the Parameters Involved in Simple Solar Still with Inclined Yute. *Renewable Energy, 14*(1-4), 333-338. https://doi.org/10.1016/S0960-1481(98)00086-X.

Faria, E.V. (2015). Simulação e análise de sistemas de destilação solar passiva (in Portuguese). Trabalho de conclusão de curso em Engenharia Química, Universidade Federal do Triângulo Mineiro, Uberaba, MG.

Freire de Sá, L. (2008). Evaporação Natural do Lixiviado do Aterro da Muribeca Através de Um Destilador Solar. Mestrado em Engenharia Civil, Universidade Federal de Pernambuco, Pernambuco, PE.

Gnanadason, M.K., Kumar, P.S., Gopal, S., & Daniel, J.E.S. (2011). Design and Performance Analysis of a Modified Vacuum Single Basin Solar Still. *Smart Grid and Renewable Energy, 2*, 388-395. https://doi.org/10.4236/sgre.2011.24044.

GOV. (2021). Matriz energética. Energia renovável chega a quase 50% da matriz elétrica brasileira (in Portuguese). [Online] Available at: https://gov.br [accessed 21 October 2022].

Incropera, F.P., Bergman, T.L. and DeWitt, D.P. (2008). *Fundamentos de Transferência de Calor e de Massa* (6th ed.). Rio de Janeiro: LTC.

Jorge, B. (2011). Simulação de processos de destilação solar de água salgada (in Portuguese). Mestrado em Engenharia Mecânica, Instituto Superior Técnico – Universidade Técnica de Lisboa, Lisboa.

Luna, F.M. (2016). Desenvolvimento e testes de um dessalinizador solar com pré-aquecimento de água (in Portuguese). Mestrado em Energias Renováveis, Universidade Federal da Paraíba, João Pessoa.

Maddah, H.A. (2019). Modeling and Designing of a Novel Lab-scale Passive Solar Still. *Journal of Engineering and Technological Sciences, 51*(3), 303-322. http://dx.doi.org/10.5614/j.eng.technol.sci.2019.51.3.1.

Maluf, A.P. (2005). Destiladores solares no Brasil (in Portuguese). Dissertação de Especialização em Fontes Alternativas de Energia, Universidade Federal de Lavras, Lavras, MG.

Mohsenzadeh, M., Aye, L. and Christopher, P. (2022). Development and validation of transient model for a passive solar still considering the aspect ratio of the evaporation chamber. *Solar Energy, 244*(15), 434-447. http://dx.doi.org/10.1016/j.solener.2022.08.059.

Moura, A.F. (2019). Modelagem e simulação numérica de um destilador solar passivo (in Portuguese). Mestrado em Engenharia Química, Universidade Federal de Viçosa, Viçosa, MG.

Panchal, H.N. and Shah, P.K. (2011). Effect of Varying Glass Cover Thickness on Performance of Solar Still in Winter Climate Conditions. *International Journal of Renewable Energy Research, 1*(4), 212-223. https://doi.org/10.20508/ijrer.v1i4.65.g58.

Raj, S.V. and Manokar, A.M. (2017). Design and Analysis of Solar Still. *Materials Today: Proceedings, 4*(8), 9179–9185. https://doi.org/10.1016/j.matpr.2017.07.275.

Silva, L., Ribeiro, M.B.M., Oliveira, A.D., Silva, C.S., Faria, E.V., & Santos, K.G. (2019). Destilação solar do solvente etanol proveniente da extração de óleo de coco (in Portuguese). *Brazilian Journal of Development, 5*, 28964-28982. https://doi.org/10.34117/bjdv5n12-066.

Singh, G., Kumar, S. and Tiwari, G.N. (2011). Design, Fabrication and Performance Evaluation of a Hybrid Photovoltaic Thermal (PVT) Double Slope Active Solar Still. *Desalination, 277*(1-3), 399–406. https://doi.org/10.1016/j.desal.2011.04.064.

Singh, G., Singh, P.K., Saxena, A., Kumar, N. and Singh, D.B. (2024). Investigation of Conical Passive Solar Still by Incorporating Energy Metrics, Efficiency, and Sensitivity Analyses for Sustainable Solar Distillation. *Journal of Cleaner Production, 434*, 139949. https://doi.org/10.1016/j.jclepro.2023.139949.

Soares, C. (2004). Tratamento de água unifamiliar através da destilação solar natural utilizando água salgada, salobra e doce contaminada (in Portuguese). Mestrado em Engenharia Ambiental, Universidade Federal de Santa Catarina, Florianópolis, SC.

Spirandeli, A.B.L., Prado, G.O. and Sousa, N.G. (2017). Desenvolvimento de um destilador solar tipo escada e análise de desempenho em relação a um destilador solar com cobertura piramidal (in Portuguese). Congresso Brasileiro de Engenharia Química em Iniciação Científica, UFSCar, São Carlos, SP.

Tanaka, H. (2009). Experimental Study of a Basin Type Solar Still with Internal and External Reflectors in Winter. *Desalination, 249*(1), 130–134. https://doi.org/10.1016/j.desal.2009.02.057.

Tayeb, A.M. (1992). Performance Study of Some Designs of Solar Stills. *Energy Conversion and Management, 33*(9), 889–898. https://doi.org/10.1016/0196-8904(92)90018-R.

Trieb, F. (2007). Concentrating Solar Power for Seawater Desalination. Stuttgart, BW, Germany.

Vasconcelos, A.B. (2015). Utilização de um destilador solar convencional para o tratamento de efluente de uma agroindústria (in Portuguese). Trabalho de conclusão de curso em Engenharia Ambiental, Universidade Tecnológica Federal do Paraná, Madianeira, PR.

Villalva, M.G. and Gazoli, J.R. (2012). *Energia Solar Fotovoltaica: Conceitos e Aplicações* (in Portuguese). São Paulo: Ed. Eletrônica.

Vorayos, N. and Kiatsiriroat, T. (2006). Performance Analysis of Solar Ethanol Distillation. *Renewable Energy, 31*, 2543–2554. https://doi.org/10.1016/j.renene.2006.01.016.